Identification and quantification of flavonoids in 207 cultivated lotus (*Nelumbo nucifera*) and their contribution to different colors

Jing Liu [1] , **Yuetong Yu** [1] , **Gangqiang Dong** [2] , **Chenyang Hao** [1] , **Yan Liu** [Corresp., 1] , **Sha Chen** [Corresp. 1]

[1] China Academy of Chinese Medical Sciences, Beijing, China

[2] Amway (China) Botanical R&D Centre, wuxi, Jiangsu

Corresponding Authors: Yan Liu, Sha Chen
Email address: yliu1980@icmm.ac.cn, schen@icmm.ac.cn

Sacred lotus (*Nelumbo nucifera*) is a large economic crop, which is also cultivated as a horticultural crop. This study performed a systematic qualitative and quantitative determination of five anthocyanins and 18 non-anthocyanin flavonoids from the petals of 207 lotus cultivars. Among the compounds identified in this study, quercetin 3-*O*-pentose-glucuronide, quercetin 7-*O*-glucoside, laricitrin 3-*O*-hexose, and laricitrin 3-*O*-glucuronide were discovered for the first time in sacred lotus. The relationships between these pigments and petals colors were also evaluated. A decrease in the total content of anthocyanins and increase in the content of myricetin 3-*O*-glucuronide resulted in a lighter flower color. Furthermore, petals were yellow when the content of quercetin 3-*O*-neohesperidoside and myricetin 3-*O*-glucuronide were increased, whereas petals were red when the total anthocyanin content was high and the quercetin 3-*O*-sambubioside content was low. These investigations contribute to the understanding of mechanisms that underlie the development of flower color and provide a solid theoretical basis for the further study of sacred lotus.

1 # Identification and quantification of flavonoids in 207 cultivated lotus

2 # (*Nelumbo nucifera*) and their contribution to different colors

3 **Jing Liu[1], Yuetong Yu[1], Gangqiang Dong[2], Chenyang Hao[1], Yan Liu[1,*], Sha Chen[1,*]**

5 *[1] Key Laboratory of Beijing for identification and safety evaluation of Chinese medicine,*

6 *Institute of Chinese Materia Medica, China Academy of Chinese Medical Sciences, No.16,*

7 *Nanxiaojie, Dongzhimennei, Beijing 100700, China*

8 *[2] Amway (China) Botanical R&D Centre, Wuxi 214115, China*

10 Corresponding Author:

11 Sha Chen, schen@icmm.ac.cn and Yan Liu, yliu1980@icmm.ac.cn

13 ## Abstract

14 Sacred lotus (*Nelumbo nucifera*) is a large economic crop, which is also cultivated as a

15 horticultural crop. This study performed a systematic qualitative and quantitative determination

16 of five anthocyanins and 18 non-anthocyanin flavonoids from the petals of 207 lotus cultivars.

17 Among the compounds identified in this study, quercetin 3-*O*-pentose-glucuronide, quercetin 7-

18 *O*-glucoside, laricitrin 3-*O*-hexose, and laricitrin 3-*O*-glucuronide were discovered for the first

19 time in sacred lotus. The relationships between these pigments and petals colors were also

20 evaluated. A decrease in the total content of anthocyanins and increase in the content of

21 myricetin 3-*O*-glucuronide resulted in a lighter flower color. Furthermore, petals were yellow

22 when the content of quercetin 3-*O*-neohesperidoside and myricetin 3-*O*-glucuronide were

23 increased, whereas petals were red when the total anthocyanin content was high and the

24 quercetin 3-*O*-sambubioside content was low. These investigations contribute to the

25 understanding of mechanisms that underlie the development of flower color and provide a solid

26 theoretical basis for the further study of sacred lotus.

27 ## Introduction

28 Sacred lotus (*Nelumbo nucifera*) is a large economic crop that is also cultivated as a

29 horticultural crop; its seeds and underground stems are commonly used as vegetables, and its

30 flower has an ornamental value. It has a long cultivated history with a rich variety resource.

31 Based on morphological characteristics (Guo, 2009; Mukherjee et al., 2009), more than 500

32 cultivars of *N. nucifera* exist and are native to Asia and Australia, while *N. lutea* has yellow

33 petals and is native to North America. It is acknowledged that sacred lotus petals present

34 different colors, including red, pink, yellow, white, and red/white pied. The lotus cultivars,

35 "Feihong" "Fenhonglingxiao" "Guoqinghong" "Honghuajianlian" "Shaoxinghonglian" and

36 "Yanyangtian", attract widespread attention because of their bright red, while "Yuwan" "Xueju"
37 "Baijunzixiaolian" and "Baixuegongzhu" are loved by people owing to their pure white color. It
38 is worth mentioning that yellow occupies a special position in lotus flower colors, mainly from
39 "Meizhouhuanglian" and its hybrid descendants. Moreover, anthocyanins are known to be the
40 key factors in the diversity of sacred lotus colors (Deng et al., 2013; Yang et al., 2009). Because
41 of the presence of anthocyanins and non-anthocyanin flavonoids, lotus exhibit many beneficial
42 biological activities, such as antioxidant, anti-inflammatory, antibiotic, antiallergic and antitumor
43 activities. (Chen et al., 2012; Jung, 2008; Jung et al., 2003; Juranić and Žižak, 2005; Zhu et al.,
44 2013).

45   Deng et al. (2013) systematically analyzed the composition and content of anthocyanins,
46 flavones, and flavonols in 108 sacred lotus cultivars with different petals colors. Furthermore,
47 Chen et al. (2013) proposed a putative flavonoid biosynthetic pathway in sacred lotus; however,
48 a branch of the suggested pathway remains incomplete. To explore the flower coloration
49 mechanism in sacred lotus, Deng et al. (2015) conducted a comparative proteomics analysis of
50 petals from red and white cultivars and found that different methylation intensities on the
51 promotor sequences of the anthocyanin synthase gene may contribute to the diversity of petal
52 colors. In addition, Sun et al. (2016) validated that *NnMYB5* is a transcription activator of
53 anthocyanin synthesis and the color difference between red and yellow sacred lotus species may
54 be related to a variation in the *MYB5* gene. These studies have shown that it is pertinent to
55 investigate the mechanism that underlies color formation in sacred lotus and further study is
56 required.

57   **It appears that a correlation between chemical composition and color phenotype may**
58 **exist in sacred lotus.** To further investigate the coloring mechanism of sacred lotus petals, a
59 large number of sacred lotus samples were collected from all over the world, comprising
60 examples of almost all the colors that exist in this species. Based on this collection, we
61 systematically detected, qualified, and quantified the contents of anthocyanins and non-
62 anthocyanin flavonoids in 207 sacred lotus cultivars, and measured the petal color phenotypes
63 using spectrophotometry. In addition, correlations between petal color and the presence of
64 different pigments were analyzed. This work may benefit our understanding of the relationship
65 between the composition of flavonoids and petal color in sacred lotus, while providing a basis for
66 subsequent research on this important plant species.

Materials & Methods

68 **Chemicals and materials**
69   The anthocyanin standard petunidin 3-*O*-glucoside (≥98.0%) and flavonol standards
70 hyperoside, astragalin, and isorhamnetin 3-*O*-glucoside (≥98.0%) were purchased from Chengdu
71 Push Bio-technology Co., Ltd. Acetonitrile and formic acid were obtained from Sigma-Aldrich
72 (St. Louis, MO, USA), which were applied as eluent and eluent additive in ultra high-
73 performance-liquid chromatography (UPLC) and UPLC-mass spectrometry (UPLC-MS). Other
74 analytical grade reagents were purchased from the Beijing Chemistry Factory (Beijing, China).

75 UPLC-grade water was obtained from Watsons water. Millipore membranes (0.22 μm) were
76 acquired from Alltech Scientific (Beijing, China). The samples were powdered in liquid nitrogen
77 using an analytical mill (IKA A11 basic machine, Germany).

Plant materials

79 Petals of 207 sacred lotus cultivars (**Supplementary Table S1**) were grown in the United
80 Lotus Germplasm Resource of the Amway Plant Research and Development Center and the
81 Chinese Academy of Traditional Chinese Medicine (China, WuXi, lat. 31º57', N long, 120º 29')
82 in the same-sized containers (height: 90 cm, diameter: 70 cm), while receiving the same
83 fertilization and disease control treatments. Two days after the bracts emerged, three biological
84 replicates of petals from each cultivar were manually collected, during May and June of 2018
85 (ambient temperature, 26–30ºC), from three individual plants. The fresh petals were immediately
86 frozen in liquid nitrogen, powdered with an analytical mill (IKA AII basic, IKA), and then stored
87 at -80°C until later use.

Color analysis

89 The fresh petals were compared to the Royal Horticultural Society Color Chart (RHSCC)
90 and sorted into four color groups, including purple-red, red, yellow, and white. The colors of the
91 lotus flowers were measured using a spectrophotometer (NF555, Nippon Denshoku, Japan). For
92 each lotus flower, petals were randomly selected, except for those in the outermost and
93 innermost layers. The selected petals were then measured at a viewing angle of 2° under
94 Illuminant C. And ColorMate software (version 5) was adopted to collect and process the values
95 of $L*$, $a*$, $b*$, $C*$, and h. The $L*$ value symbolizes the lightness of the color. With L value
96 increased, the color becomes lighter, from black ($L* = 0$) to white ($L* = 100$). In addition,
97 positive and negative $a*$ values separately represent red and green, while positive and negative
98 $b*$ values on behalf of yellow and blue, respectively. Two new parameters, chroma [$C* = (a^{*2} +$
99 $b^{*2})^{1/2}$] and hue angle [$h = \arctan b*/a*$], were derived from $a*$ and $b*$. The chroma parameter
100 describes the saturation of the color, while the hue angle value is stepped counterclockwise
101 across a continuously fading hue circle (Gonnet, 1998, 1999). The co-pigment index (CI) value
102 [$CI = TF/TA$], which represents the co-pigmentation effect, is calculated from the total content of
103 non-anthocyanin flavonoids (TF) and the total content of anthocyanins (TA). TF and TA will be
104 described in the section "Anthocyanin and non-anthocyanin flavonoid profiles in sacred lotus
105 petals".

Extraction of anthocyanins and non-anthocyanin flavonoids

107 The petals were ground into fine powders in liquid nitrogen using an analytical mill (IKA
108 A11 basic machine, Germany). All of the collected samples were extracted according to the
109 method reported by Deng et al. (2013) and Chen et al. (2013), with the following modifications:
110 a solvent system comprising methanol, water, and formic acid (70:28:2, v:v:v) was applied in the
111 extraction, and 1 g of sacred lotus petals was extracted with 8 mL of extraction buffer and
112 sonicated for 20 min at room temperature. The extracts were centrifuged at 5000 × g for 10 min,
113 and the supernatants filtered through a 0.22 μm Millipore filter (Alltech Scientific Corporation)
114 prior to UPLC analysis.

HPLC analysis of flavonoids

115 The analysis of flavonoids was carried out using a Waters H-Class UPLC system consisting
116 of an auto-sampler and quaternary pump arrangement (Waters Corporation, USA) coupled to a
117 UV–vis detector. Compared with previous reports (Chen et al., 2012; Lin and Harnly, 2007;
118 Nováková et al., 2006), our UPLC method showed higher separation efficiency and resulted in a
119 shorter run-time. A 5 μl aliquot of each sample solution was injected and analyzed on a Waters
120 Xselect C_{18} column (150 mm × 4.6 mm, 3.5 μm, Waters, USA). In the solvent system, eluent A
121 was 10% formic acid in water and eluent B was 0.1% formic acid, added in acetonitrile, as the
122 organic phase. Chromatograms were acquired at 520 nm and 350 nm for anthocyanins and non-
123 anthocyanin flavonoids, respectively. The gradient elution conditions for the separation of the
124 extracted flavonoids were as follows: 0-10 min, 8-15% B; 10-19 min, 15-21% B; 19-22 min,
125 21% B; 22-23 min, 21-98% B; 23-35 min, 98% B; 35-35.1 min, 98-8% B; 35.1-50 min, 8% B;
126 flow rate, 0.5 mL min^{-1}; and temperature, 30℃.
127 Anthocyanins and non-anthocyanin flavonoids were quantitatively analyzed with reference
128 to external standards (petunidin 3-O-glucoside and hyperoside). The calibration curves showed
129 good linear regression within test concentration ranges, with $R^2 = 0.9972$ and 0.9994,
130 respectively. The limits of detection of the optimized method, calculated as a signal-to-noise
131 ratio of three, were 0.059 μg mL^{-1} and 0.016 μg mL^{-1} for petunidin 3-O-glucoside and
132 hyperoside, respectively, while the limits of quantification, with a signal-to-noise ratio of 10,
133 were 0.228 μg mL^{-1} and 0.063 μg mL^{-1}, respectively. In addition, the newly developed method
134 provided satisfactory precision and accuracy with overall intra-day and inter-day variations of
135 0.09–3.41% and 0.66–3.91%, respectively. These results indicated that the optimized UPLC
136 method was stable and suitable for use in the quantitative analysis of flavonoids in sacred lotus
137 petals. In addition, content of compounds **3**, **11**, **19**, and **21** were quantified by comparison with
138 external standards, while compounds **1**, **2**, **4**, and **5** are given in ug/g FW equivalent of petunidin
139 3-O-glucoside. The other non-anthocyanin flavonoids were quantified as hyperoside.

UPLC-ESI-Q-TOF-MS/MS analysis for determination of flavonoids

142 Flavonoids in the sacred lotus petal extracts were identified using an Agilent 1290
143 photodiode array and 6540 triple quad mass time-of-flight (Q-TOF) mass spectrometer, equipped
144 with a dual electrospray ionization (ESI) detector (Agilent, Palo Alto, CA, USA). Nitrogen
145 auxiliary gas was provided. ESI was performed in the negative ionization (NI) mode for both MS
146 and tandem MS (MS/MS) analysis to provide fragmentation information about the molecular
147 weights of the molecules being screened. The ESI source operation parameters were optimized
148 as follows: gas temperature, 350℃; drying gas, 8 L min^{-1}; nebulizer, 45 psig; sheath gas temp,
149 350℃; sheath gas flow, 11 L min^{-1}; Vcap, 3500 V; nozzle voltage, 1500 V; and scan range, m/z
150 100–1100 units. A collision energy of 20 eV was used during MS/MS analysis. Purine and HP-
151 0921 were used as internal references in real time and, in NI mode, their m/z ratios were
152 119.0363 and 1033.9881, respectively. The MS data, retention times, and UV–vis spectra were
153 used to identify the flavonoids contained in the sacred lotus petals.

RNA extraction and qRT-PCR analysis

155 Total RNA was isolated from petals (B88, white petal; A89, yellow petal; B121, red petal)
156 using RNA Easy Fast Plant Tissue Kit purchased from TIANGEN BIOTECH CO., LTD
157 (Beijing, China). Each RNA sample was treated with RNase-free DNase I (TaKaRa) prior to the
158 reverse transcription (RT) reaction to eliminate contaminating genomic DNA. RT-PCR was
159 performed on the basis of the standard instruction of Prime Script RT Reagen Kit with gDNA
160 Eraser (TaKaRa).
161 As previously described in Sun et al., 2016, the qRT-PCR was carried out using Step One
162 Real-Time PCR system (Applied Biosystems, Foster City, CA, USA). A total reaction volume of
163 25 uL was applied, containing 10 uL of 2 x TransStart Green PCR Supermix UDG (S602,
164 TRANS), 4 uM of each primer, and about 100 ng of template cDNA. And the amplification
165 condition was follows: incubation at 95 ^{o}C for 2 min, denaturation at 95 ^{o}C for 5 s, annealing at
166 60 ^{o}C for 10 s, and extension at 72 ^{o}C for 10 s, and the process continued for a total of 40 cycles.
167 Besides, action gene of lotus (GenBank ID:EU131153) served as a constitutive control. Target
168 gene relative expression levels were calculated by $2^{-\triangle\triangle Ct}$ comparative threshold cycle (Ct)
169 method, and three biological replicates were conducted. Primer sequences (**Supplementary**
170 **Table S2**) were designed on the whole-genome resequencing data of *N. nucifera* (-30X coverage
171 depth). Three main genes in flavonoid biosynthesis pathway of lotus (DFR (Gene_ID:
172 NW_010729118.1_renew:02005922_02019073), UFGT (Gene_ID:
173 NW_010729304.1_renew:00079217_00080656), OMT (Gene_ID:
174 NW_010729121.1_renew:03748642_03755897) by quantitative reverse transcription –PCR
175 (qRT-PCR) were investigated.
176 **Statistical analysis**
177 Data were analyzed using SPSS 24.0 for Windows®. The color parameters and pigment
178 contents of petals from 207 cultivars were compared by analysis of variance, combined with
179 Duncan's multiple range tests. Multiple linear regressions (MLR) were established to study the
180 interactions between pigment compositions and color formation.

181 # Results

182 **Identification of anthocyanins and non-anthocyanin flavonoids**
183 Flavonoids were identified according to the accurate molecular and fragment ion
184 information obtained using MS and MS/MS, UV–vis spectra, and retention times on the C18
185 column, as revealed by HPLC and HPLC-MS. Ultimately, five anthocyanins and 18 non-
186 anthocyanin flavonoids were identified (**Table 1, Figure 1A**). Flavonoids glycosylated with
187 monosaccharide glycosides show mass spectrometric behavior when using MS with ESI in NI
188 mode. As reported (Ablajan et al., 2006), when the abundance of the radical aglycone, annotated
189 as [A−2H]−, is notably higher than that of the aglycone product ion, annotated as [A−H]−, the
190 glycoside is usually linked at the 3-position, and the opposite abundance trend occurs when the
191 conjugation occurs at the 7-position. However, as an exception, only the aglycone product ion
192 can be produced when there is a glucuronic acid group, no matter whether the linked position is 3
193 or 7. The neutral loss of fragment ions of 146 and 176 mass units, which were produced by the

194 protonated precursor 623.1475 [M-H]- for peak 8, implied that a pentose and a glucuronide were
195 linked at the 3-position. Moreover, the aglycone product ion at m/z 301.0467 [A-H]- in NI mode
196 indicated that the flavonoid aglycone is quercetin, and thus peak 8 was tentatively identified as
197 quercetin 3-*O*-pentose-glucuronide (Qc-3-Pen-Gln) (**Figure 1B**). As regard to the peak 9, due to
198 the neutral loss of a fragment ion of 162 mass units, which was produced by the protonated
199 precursor of 463.0910 [M-H]-, and the intensive showing of an aglycone product ion at m/z
200 301.0362 [A-H]- indicated that the linked position is 7 (**Figure 1C**), thus peak 9 was temporarily
201 identified as quercetin 7-*O*-glucoside (Qc-7-Glu). Furthermore, based on the MS/MS spectra
202 data, both peak 13 and peak 14 were tentatively assigned as laricitrin monosaccharide, which has
203 been reported in grapes (Jin et al., 2009). The radical aglycone ion at m/z 330.0482 [A-2H]- and
204 the corresponding ion at m/z 315.0228 [A-2H-CH$_3$]-, with a fragment ion of 163 mass units,
205 demonstrated that a hexose substituent was linked at the 3-position (**Figure 1D**). Hence, peak 13
206 was tentatively identified as laricitrin 3-*O*-hexose (Lar-3-hex); and further work is required to
207 identify the nature of this hexose-based compound. Meanwhile, according to the data acquired
208 for the glycone product ion at m/z 331.0581 [A-H]-, and the protonated precursor of 507.0999
209 [M-H]-, the loss of a fragment ion of 176 mass units manifested that a glucuronic acid glycoside
210 was conjugated at the 3-position. In addition to the corresponding ion at m/z 316.0342 [A-H-
211 CH$_3$]- (**Figure 1E**), peak 14 was assigned as laricitrin 3-*O*-glucuronide (Lar-3-Gln).
212   The chromatographic and MS data for the anthocyanins and non-anthocyanin flavonoids
213 separated and identified from the sacred lotus petals are listed in **Table 1**. The data from the MS
214 analysis in NI mode provided valuable information, including molecular weights and information
215 about the presence of aglycones and sugars, with their linkage positions. Peaks 1-5 were
216 identified as the following anthocyanins: delphinidin 3-*O*-glucoside (Dp-3-Glu, **1**), cyanidin 3-*O*-
217 glucoside (Cy-3-Glu, **2**), petunidin 3-*O*-glucoside (Pt-3-Glu, **3**), peonidin 3-*O*-glucoside (Pn-3-
218 Glu, **4**), and malvidin 3-*O*-glucoside (Mv-3-Glu, **5**), as previously reported (Yang et al., 2009).
219 Peaks 6-23 were identified as non-anthocyanin flavonoids: myricetin 3-*O*-glucuronide (Myr-3-
220 Gln, **6**) (Deng et al., 2013), quercetin 3-*O*-xylopyranosyl-(1→2)-glucopyranoside (quercetin 3-
221 *O*-sambubioside/Qc-3-Sam, **7**) (Deng et al., 2009), quercetin 3-*O*-pentose-glucuronide (Qc-3-
222 Pen-Gln, **8**), quercetin 7-*O*-glucoside (Qc-7-Glu, **9**), quercetin 3-*O*-rhamnopyranosyl-(1→2)-
223 galactopyranoside (quercetin 3-*O*-neohesperidoside/Qc-3-Neo, **10**) (Li et al., 2014b), quercetin
224 3-*O*-galactoside (Qc-3-Gal/Hyperoside, **11**) (Suzuki et al., 2008), quercetin 3-*O*-glucuronide
225 (Qc-3-Gln, **12**) (Yang et al., 2009), laricitrin 3-*O*-hexose (Lar-3-hex, **13**), laricitrin 3-*O*-
226 glucuronide (Lar-3-Gln, **14**), kaempferol 3-*O*-rhamnopyranosyl-(1→2)-glucopyranoside
227 (kaempferol 3-*O*-neohesperidoside/Kae-3-Neo, **15**) (Lim et al., 2006; Sharma et al., 2017),
228 kaempferol 3-*O*-galactoside (Kae-3-Gal, **16**) (Jung et al., 2003), kaempferol 3-*O*-
229 rhamnopyranosyl-(1→6)-glucopyranoside (kaempferol 3-*O*-rutinoside/Kae-3-Rut, **17**) (Hyun et
230 al., 2017; Sharma et al., 2017), isorhamnetin 3-*O*-rutinoside (Iso-3-Rut, **18**) (Yang et al., 2009),
231 kaempferol 3-*O*-glucoside (Kae-3-Glu/astragalin, **19**) (Chen et al., 2012; Yang et al., 2009),
232 syringetin 3-*O*-hexose (Syr-3-Hex, **20**) (Guo, 2009), isorhamnetin 3-*O*-glucoside (Iso-3-Glu, **21**)
233 (Sharma et al., 2017), isorhamnetin 3-*O*-glucuronide (Iso-3-Gln, **22**) (Chen et al., 2012), and

234   syringetin 3-*O*-glucuronide (Syr-3-Gln, **23**) (Li et al., 2014b). These 18 non-anthocyanin
235   flavonoids were classified into six groups: quercetin (Qc), kaempferol (Kae), isorhamnetin (Iso),
236   myricetin (Myr), syringetin (Syr), and laricitrin (Lar), based on the aglycones they contain.
237   In this study, the four non-anthocyanin flavonoids discussed above (**Figure 1**), including
238   Qc-3-Pen-Gln (**8**), Qc-7-Glu (**9**), Lar-3-Hex (**13**) and Lar-3-Gln (**14**), were discovered for the
239   first time in sacred lotus petals using the newly developed UPLC-DAD-ESI-Q-TOF-MS/MS
240   technique. Therefore, our study has further refined the research carried out by Chen et al. (2013)
241   and Deng et al. (2013).

242   **Anthocyanin and non-anthocyanin flavonoid profiles in sacred lotus petals**

243   By comparison with the RHSCC, the 207 sacred lotus cultivars were grouped into four
244   color groups: purple-red, red, yellow, and white. Although there were five different anthocyanins
245   and 18 non-anthocyanin flavonoids detected in the flower petals, the compositions and total
246   contents varied significantly among different cultivars. The most abundant anthocyanin was Mv-
247   3-Glu (**5**), which accounted for 50% of the compounds in the purple-red group and 47% of those
248   in the red group. This was followed by Dp-3-Glu (**1**), which accounted for 19% of the
249   compounds in the purple-red group and 17% of those in the red group. As for the non-
250   anthocyanin flavonoids, quercetin-, kaempferol-, and isorhamnetin-derivatives were the
251   dominant non-anthocyanin flavonoids in all of the four color groups; however, quercetin
252   derivatives were the most abundant (**Supplementary Figure S1**). Of note, in yellow cultivars,
253   quercetin derivatives were seen to be the most important flavonoids, as these were present in
254   significantly higher amounts (up to 64%) than the other five flavone aglycone derivatives,
255   suggesting a link between these compounds and the yellow petal color. Additionally, kaempferol
256   and isorhamnetin derivatives were the second and third most abundant complexes in yellow
257   petals, accounting for 16% and 9% of the TF, respectively. Conversely, quercetin and
258   kaempferol derivatives showed equal importance in their contribution to the TF of the purple-
259   red, red, and white color groups, making up approximately 85% of the TF (**Table 2**). Among all
260   the cultivars tested, the highest TA was detected in cultivars of the purple-red group, with a mean
261   content of 464.47 ug/g fresh weight (FW), followed by the red group, with an average content of
262   171.74 ug/g FW. Generally, the petals containing more anthocyanins displayed darker colors; for
263   example, the purple-red cultivar 'Cuifuhongya' (27) had the highest mean anthocyanin content
264   (1133.61 ug/g FW) among all the cultivars. In terms of germplasm assessment, some cultivars,
265   such as 'Qiuwanluoshan' (5), 'Ti-13' (74), and 'Ti-13-I' (9), which contain very high contents of
266   Mv-3-Glu (**5**) and relatively higher TA, may be ideal candidates for breeding purple-red flowers
267   and studying the anthocyanin biosynthesis pathway in sacred lotus. What's more, the TF was the
268   highest in yellow petals, with an average content of 3517.93 ug/g FW. The yellow petal cultivar
269   'Jintaiyang' (165) contained the highest TF, with a concentration of 7149.35 ug/g FW, and
270   would be a candidate cultivar for the study of the coloring mechanism in yellow sacred lotus
271   (**Figure 2**).

272   What's more, significant differences were observed in the contents of anthocyanins and
273   non-anthocyanin flavonoids among cultivars of differing color. In order to visualize these

274   differences, individual anthocyanin and non-anthocyanin flavonoid contents were normalized

275   using the Z-score and expressed as a heat map (**Figure 3**). In purple-red cultivars, Mv-3-Glu (**5**)

276   and Dp-3-Glu (**1**) were the two major anthocyanins, while Qc-3-Gln (**12**) and Kae-3-Glu (**19**)

277   were the two dominant non-anthocyanin flavonoids. The red cultivars exhibited similar profiles,

278   with Mv-3-Glu (**5**) being the most highly concentrated anthocyanin, with Qc-3-Gln (**12**) and

279   Kae-3-Glu (**19**) the most abundant non-anthocyanin flavonoids. The yellow and white cultivars,

280   however, demonstrated a deficiency of anthocyanins and an abundance of non-anthocyanin

281   flavonoids. In yellow cultivars, the concentration of Qc-3-Gln (**12**) was found to be the greatest

282   among the 18 non-anthocyanin flavonoids, which may contribute to the yellow color.

283   Furthermore, the concentrations of Myr-3-Gln (**6**), Qc-3-Neo (**10**), Qc-3-Gal (**11**), Iso-3-Glu

284   (**21**), Iso-3-Gln (**22**), Syr-3-Gln (**23**), Syr-3-Hex (**20**), and Iso-3-Rut (**18**) showed varying degrees

285   of increase, in association with purple-red and red colored cultivars. In white cultivars, the TF

286   exhibited similar trends to those of the yellow cultivars, but at relatively lower levels.

287   Differences in the distribution of the contents of these ingredients suggested that the color of the

288   sacred lotus may be related to a single anthocyanin or non-anthocyanin flavonoid.

289   **Relationships between petal color, anthocyanins, and non-anthocyanin flavonoids**

290   Researchers have reported that flavones and flavonols are responsible for flower color (Li et

291   al., 2008), but the relationships between these factors are unknown in sacred lotus. In maize,

292   non-anthocyanin flavonoids are considered to be co-pigments, alongside anthocyanins (Stafford,

293   1998). Hence the co-pigmentation index is an important indicator of the co-pigmentation effect,

294   which occurs, in the main, when CI > 5 (Asen et al., 1971; He et al., 2011). According to the

295   formula CI = TF/TA, we found that, in the most purple-red sacred lotus petals, CI was <5, while

296   in the other three color groups, CI tended to be >5, indicating that non-anthocyanin flavonoids

297   had a significant effect on the color of sacred lotus petals, especially when the anthocyanin

298   content was low. This result was in line with the suggestion that co-pigmentation between

299   anthocyanins and non-anthocyanin flavonoids may result in distinct petal colors (Li et al., 2011;

300   Zhang et al., 2011b; Zhu et al., 2012).

301   To analyze the relationship between petal color and pigment content in sacred lotus,

302   Pearson's correlation coefficients were calculated among color parameters, anthocyanin

303   contents, and non-anthocyanin flavonoids contents, and displayed as a heat map (**Figure 4**).

304   Strong correlations were seen. For example, L* values were significantly negatively correlated

305   with a*, C*, and h ($P < 0.01$), and significantly positively correlated with b* and CI ($P < 0.01$).

306   The individual anthocyanin contents of the five groups and TA demonstrated significant negative

307   correlations with L*, b*, and CI ($P < 0.01$), and positive correlations with a*, C*, and h ($P <$

308   0.01). In addition, TF, and most of the individual non-anthocyanin flavonoid contents, were

309   negatively correlated with a*, C*, and h, but positively correlated with L*, b*, and CI. Moreover,

310   Qc-3-Neo (**10**), Qc-3-Gal (**11**), Kae-3-Rut (**17**), Iso-3-Rut (**18**), Syr-3-Hex (**20**), Iso-3-Gln (**22**),

311   and Syr-3-Gln (**23**)were significantly correlated with all of the six color parameters (L*, a*, b*,

312   C*, h, and CI), while Qc-3-Pen-Gln (**8**) and Kae-3-Glu (**19**) had no apparent correlations with

313   most of these color parameters. Correlations among anthocyanin and non-anthocyanin flavonoid

314   metabolism were also evaluated. Strong positive correlations were found between different
315   anthocyanins ($P < 0.01$) and between different non-anthocyanin flavonoids. However, significant
316   negative correlations were observed between anthocyanins and most non-anthocyanin flavonoids
317   ($P < 0.05$), as was found for TA and TF. The correlation analysis indicated that many pigments
318   influence sacred lotus petal color. Thus, MLR analysis was used to estimate the type of pigment
319   that dramatically affects petal color. Color parameters, including L*, a*, and b*, were chosen as
320   dependent variables, and 25 indexes, containing 23 various pigment components, plus TA and
321   TF, were selected as independent variables. To study the interactions between these pigment
322   compositions and color formation, regression equations were established. Significant statistical
323   results were acquired as follows:

324   L* = 76.083 - 0.028 TA + 0.022 Myr-3-GlcA (**6**) ($R^2 = 0.408$, P = 3.008E-24)

325   a* = 15.783 + 0.052 TA - 0.575 Qc-3-Sam (**7**) + 0.233 Kae-3-Rut (**17**) - 0.003 TF ($R^2 =$
326   0.630, P = 1.079E-42)

327   b* = 0.719 + 0.219 Qc-3-Neo (**10**) + 0.033 Myr-3-GlcA (**6**) + 0.121 Syr-3-GlcA (**23**) -
328   0.196 Pn-3-Glc (**4**) - 0.325 Syr-3-Hex (**20**) ($R^2 = 0.570$, P = 1.006E-35)

329   The MLR analysis showed that there are many factors affecting petal color, including TA,
330   TF and the levels of Myr-3-GlcA (**6**), Qc-3-Sam (**7**), Kae-3-Rut (**17**), Qc-3-Neo (**10**), Myr-3-Gln
331   (**6**), Syr-3-GlcA (**23**), Pn-3-Glc (**4**) and Syr-3-Hex (**20**), among which, TA was the major factor,
332   with positive effects on the values of a*, but negative effects on the value of L*. Myr-3-GlcA (**6**)
333   was another important factor that exhibited positive effects on the L* value. TA was found to be
334   the primary factor positively influencing the a* value, whereas Qc-3-Sam (**7**) negatively affected
335   the a* value. Furthermore, Qc-3-Neo (**10**), Myr-3-Gln (**6**) and Syr-3-GlcA (**23**) had positive
336   effects on value of b*. Based on these findings, an increase in TA was determined to push up the
337   values of a*, but lower the value of L*, indicating that the flower colors would become red and
338   darker. The L* value indicates that with less TA and higher Myr-3-GlcA (**6**) contents, flowers
339   are lighter or white in color. Parameter a* suggests that higher TA and Kae-3-Rut (**17**) contents,
340   with lower Qc-3-Sam (**7**) contents and TF, lead to a deeper red flower color, whereas b*
341   indicates that higher Qc-3-Neo (**10**), Myr-3-Gln (**6**) and Syr-3-GlcA (**23**) levels deepen the
342   yellow color of petals. In summary, increasing the content of Myr-3-GlcA (**6**) and decreasing the
343   TA results in a lighter flower color, whereas a rise in Qc-3-Neo (**10**) and Myr-3-GlcA (**6**) turns
344   petals yellow, while a higher TA and Kae-3-Rut (**17**) contents and lower Qc-3-Sam (**7**) contents
345   turns flowers red.

346   **Putative flavonoid biosynthesis pathway of lotus**

347   In our study, 5 anthocyanins and 18 non-anthocyanin flavonoids were simultaneously
348   detected, qualified and quantified in 207 sacred lotus cultivars, among which, four components
349   were discovered for the first time in sacred lotus petals. Combined with these newly detected
350   compounds in sacred lotus petals and previous study (Chen et al., 2013; Li et al., 2014b), the
351   sacred lotus biosynthetic pathway for the detected anthocyanins and non-anthocyanin flavonoids
352   was deduced in depth (**Figure 5**). The precursors of flavonoid biosynthesis are 4-coumaroyl-

353   CoA and Malonyl-CoA, which are condensed to form Naringenin under the catalysis of chalcone

354   synthase (CHS) and chalcone isomerase (CHI). Then, with the help of flavonoid 3-hydroxylase

355   (F3H), flavonoid 3'-hydroxylase (F3'H) and flavonoid 3'5'-hydroxylase (F3'5'H),

356   dihydrokaempferol, dihydroquercetin and dihydromyricetin were synthesized, which were the

357   most essential precursor compounds used to synthesize the corresponding anthocyanins and non-

358   anthocyanin flavonoids. As the biosynthesis of flavonols is closely concerning to that of

359   anthocyanins (Jeong et al., 2006), the pathway then divided into five sub-pathway. Flavonol

360   synthase (FLS) played a decisive role for producing aglycones of non-anthocyanin flavonoids,

361   while dihydroflavonol reductase (DFR) determined the generation of anthocyanins. The main

362   difference is sub-pathway 3, for the presence of flavonol kaempferol synthesized from

363   dihydrokaempferol, while the anthocyanin pelargonidin is lacking in sacred lotus (Li et al.,

364   2014b). Finally, both anthocyanins and non-anthocyanin flavonoids, with the assistance of

365   enzyme UDP flavonoid glycosyltransferase (UFGT), O-methyltransferase (OMT) and other

366   enzymes, performed different structural modification at the linkage position. Especially,

367   glycosylation is a key mechanism to coordinate the bioactivity, metabolism and location of small

368   molecules in living cells (Pfeiffer & Hegedűs, 2011). As shown in our study, it may be much

369   simpler to glycosylate at 3-O-position in sacred lotus petals, with the exception of quercetin. The

370   compound Qc-7-Glu (**9**), glycosylated in the 7-O-position, was detected for the first time in

371   sacred lotus. More importantly, the first discovery of laricitrin derivatives supplemented the sub-

372   pathway 5, which was validated by the results of the large data resources and chemical

373   technologies.

374   To further valid the flavonoid biosynthetic pathway we proposed, total RNA was isolated

375   from three lotus cultivars with different petal colors, and qRT-PCR was conducted to observe

376   these gene expressions (DFR, OMT, UFGT) in lotus petals with different colors (**Figure 6**). The

377   qRT-PCR results showed that the expressions of DFR and UFGT in red petals was significantly

378   higher than those of yellow and white petals, indicating the higher anthocyanin content in red

379   petal cultivars. In addition, the expression levels of OMT genes in yellow petals were

380   significantly higher than those in red and white petals, suggesting the higher non-anthocyanin

381   flavonoids contents in yellow petal cultivars. The qRT-PCR results further validated the putative

382   flavonoid biosynthetic pathway.

383   **Discussion**

384   **Pigments determine the different colors of various sacred lotus cultivars**

385   Since the mid-19th century, pigments have been extracted from colorful flowers to research

386   the components, and a wide variety of pigments have been discovered, such as carotenoids and

387   flavonoids. Carotenoids are considered to be the most widely distributed pigments in nature,

388   which could not only be found in flowers, but also in fruits and storage organs in higher plants

389   (Zhu et al., 2010). Previous study showed that carotenoids existed in petals of different plant

390   species, and contributed to the yellow color, such as in *Osmanthus fragrans*, butter yellow and

391   golden yellow petals contain α-carotene and β-carotene (Han et al., 2013). The carotenoids may

392   have relationship with the yellow petals color of *N*. lutea, while the physical and chemical

393   properties of carotenoids varied greatly with the flavonoids, which need deep research,

394   separately. It is acknowledged that flavonoids are a large class of secondary metabolites, which

395   also widely distributed in lotus (Li et al., 2014a). Previous studies have shown that anthocyanins

396   belong to the red series of pigments and control flowers colors from pink to blue violet, while

397   non-anthocyanin flavonoids belong to the pure yellow series, controlling colors from deep

398   yellow to light yellow and approaching colorlessness (He et al., 2011; Zhao et al., 2012; Zhao

399   and Tao, 2015). Cyanidin appears in red flowers, while delphinidin leans petals toward the blue

400   spectrum (Sun et al., 2009; Zhang et al., 2011a). In tropical water lilies, the cultivars in which

401   delphinidin 3-galactoside was detected presented an amaranth color, whereas those containing

402   delphinidin 3'-galactoside appeared blue (Zhu et al., 2012). However, an overview of the

403   relationship between color phenotype and chemical composition remains lacking in sacred lotus.

404   In this study, 5 anthocyanins and 18 non-anthocyanin flavonoids were simultaneously detected,

405   qualified and quantified in 207 sacred lotus cultivars, with four components firstly discovered.

406   The composition and content of these anthocyanins and non-anthocyanin flavonoids were also

407   investigated in 207 lotus varieties (**Figure 2**), which can be help to screen the lotus germplasm

408   with a high content of specific secondary metabolites. In addition, statistical analysis of

409   flavonoids in lotus petals of different colors revealed that the contents of non-anthocyanins

410   flavonoids were far higher than those of anthocyanins, and the distribution of these components

411   differed significantly in lotus petals of different colors (**Table 2**). It can be seen that in lotus

412   petals, quercetin derivatives are the most prominent flavonoids with the largest accumulation,

413   which is consistent with lotus leaves (Goo et al., 2019). And the content of kaempferol

414   derivatives in lotus petals ranked second. What's more intresting is that anthocyanins are mainly

415   distributed in purple-red and red lotus cultivars, and are rarely produced in yellow and white

416   varieties. Among the five anthocyanins, malvidin 3-*O*-glucoside accumulated the highest in lotus

417   petals, followed by delphinidin 3-*O*-glucoside. However, the petals are still red rather than blue,

418   so the mechanism of lotus colors remains to be further studied. Unlike anthocyanins, no-

419   anthocyanin flavonoids existed universally in all the lotus cultivars, and accumulated the highest

420   in yellow petals. As anthocyanins and non-anthocyanin flavonoids were known to contribute a

421   lot to the lotus colors (Li et al., 2008), significance analysis was conducted, and notable

422   differences were observed in the contents of anthocyanins and non-anthocyanin flavonoids

423 among cultivars of differing color. In addition, strong correlations were seen among color

424 parameters, anthocyanin contents, and non-anthocyanin flavonoids contents (**Figure 3**). The

425 results further confirmed that there may be some intrinsic link between lotus color and pigments.

426 Moreover, MLR analysis showed that there are many factors affecting petal color of sacred lotus.

427 It is considered that TA is the essential factor responsible for sacred lotus color. With the

428 increase in TA, a* value increased and L* value decreased, indicating the intense red and dark

429 color of sacred lotus petals. In addition, Qc-3-Neo (**10**) was found to be the primary factor

430 positively influencing the b* value, suggesting the higher Qc-3-Neo (**10**) content, the deeper

431 yellow petal color. Thus, it could be speculated that red color of sacred lotus petals due to

432 anthocyanins content, while the yellow and white color are owing to non-anthocyanin flavonoids

433 content (**Figure 4**). While there are many studies using mathematical models to study flower

434 color and composition (Wang et al., 2001; Zhang et al., 2011a), rarely studies have been done in

435 this way in lotus. Our studies take advantage of large sample data to establish a mathematical

436 relationship model between lotus color parameters and active ingredients, making it more

437 digitized and visualized, which is of great significance to further research of the formation

438 mechanism of lotus color.

439 **Regulatory genes contribute to flower coloration of lotus**

440 In the present study, a model explaining the biosynthetic pathway of flavonoids in lotus was

441 proposed to give us a better understanding of the connection between flower coloration and the

442 modified patterns of anthocyanins and non-anthocyanin flavonoids (**Figure 5**). The flavonoid

443 biosynthesis pathway consists of five sub-pathways, indicating that the biosynthesis of flavonols

444 is closely related to the biosynthesis of anthocyanins. Flavonols and anthocyanins appear to

445 compete for a common substrate. Due to the different activities of flavonol synthase (FLS) and

446 dihydroflavonol reductase (DFR), the same substrate, dihydroquercetin, produces quercetin

447 (subpathway 1) and leucocyanidin (subpathway 2), respectively. In addition, it can be seen from

448 the Pearson correlation coefficient that there is a certain negative correlation between Cy-3-Glc

449 (**2**) and quercetin derivatives (**Figure 4**), further verifying the competition between sub-pathways

450 1 and 2. The rule also applies to myricetin (sub-pathway 5) and leucodelphinidin (sub-pathway

451 4). More importantly, kaempferol derivatives were not significantly different among the four

452 different colored lotus varieties (**Table 2**), possibly due to the lack of the corresponding

453 competing anthocyanin pelargonidin. To date, many studies has reported that variation in

454 regulatory genes is central to variation in pattern and intensity of pigmentation through the

455 genetic basis of flower coloration (Schwinn et al., 2006; Yamagishi et al., 2010). Sun et al.

456 identified and isolated several regulatory genes from sacred lotus, and a striking difference in

457 *MYB5* gene was detected in two sacred lotus species through introducing *NnMYB5* into

458 *Arabidopsis* plants, indicating *MYB5* is a functional transcription activator of anthocyanin

459   synthesis, and related to the flower color difference between red flowers and yellow flowers (Sun
460   et al., 2016). However, it still needs further effort to investigate the regulation mechanism of
461   flavonoid biosynthesis in sacred lotus. Based on the biosynthetic pathway of flavonoids in lotus
462   that we put forward, we further verified the expression of pathway genes in lotus petals of
463   different colors (**Figure 6**). The qRT-PCR results showed that the expression of DFR in red
464   petals was significantly higher than that of yellow and white petals, which was consistent with
465   high anthocyanin content in red petal cultivars. The expression levels of OMT genes in yellow
466   petals were significantly higher than in red and white flowers, which was consistent with high
467   non-anthocyanin flavonoids contents in yellow petal cultivars. Studies have shown that
468   modulating gene expression in the flavonoid biosynthetic pathway can alter flower color (Noriko
469   et al., 2010). Moreover, strategies to genetically engineer flower color through the flavonoid
470   biosynthetic pathway have attracted widespread attention (Nishihara et al., 2011). The results
471   suggested that essential enzymes required for regulating flavonoid biosynthesis, such as DFR
472   and OMT, can control the content of endogenous pigments in lotus petals. By manipulating
473   specific lotus flavonoid pigments, alteration in flower color is expected. Previously, we
474   sequenced these 207 sacred lotus cultivars. Combined with the metabolome data in this study,
475   the regulatory patterns and metabolic pathways of flavonoids will be further studied and the
476   relationship between the compositions of flavonoids and petal colors in sacred lotus can be
477   hopefully explained at the molecular level.

Conclusions

479   In this study, we developed an analytical method to detect a wide range of anthocyanins and
480   non-anthocyanin flavonoids simultaneously in a dramatically shortened time period in the petals
481   of 207 sacred lotus cultivars. Among the five anthocyanins and 18 non-anthocyanin flavonoids
482   identified, four of the latter were reported for the first time in sacred lotus petals. Furthermore,
483   the relationships between flower color and pigment composition and content were elucidated.
484   The results showed that Mv-3-Glu (**5**) is the dominant anthocyanin, while Qc-3-Gln (**12**)
485   accounts for most of non-anthocyanin flavonoids in sacred lotus cultivars. Moreover, there are
486   significant differences in the anthocyanin and non-anthocyanin flavonoid contents among
487   different cultivars, and MLR analysis confirmed that the TA was the most essential factor for
488   determining petal color. A higher content of Qc-3-Neo (**10**) and Myr-3-GlcA (**6**) results in
489   yellow flowers, while an increased TA and reduced Qc-3-Sam (**7**) content lend petals to turn red.
490   These results are indispensable to investigating the relationship between the compositions
491   of anthocyanins, non-anthocyanin flavonoids, and petal colors in sacred lotus. The findings will
492   contribute to our understanding of flavonoid biosynthesis, which may provide a theoretical basis
493   for developing sacred lotus petals as a natural source of anthocyanins and non-anthocyanin

494 flavonoids. In addition, this research will lay a solid foundation for subsequent investigations
495 into metabolic and biosynthetic pathways in sacred lotus.

496

References

498 Ablajan, K., Abliz, Z., Shang, X.Y., He, J.M., Zhang, R.P., and Shi, J.G. (2006). Structural
499 characterization of flavonol 3,7-di-O-glycosides and determination of the glycosylation position
500 by using negative ion electrospray ionization tandem mass spectrometry. J Mass Spectrom.
501 41(3), 352-360. doi: 10.1002/jms.995.
502 Asen, S., Stewart, R.N., and Norris K.H. (1971). Co-pigmentation effect of quercetin glycosides
503 on absorption characteristics of cyanidin glycosides and color of Red Wing azalea.
504 Phytochemistry. 10(1), 171-175. doi: 10.1016/S0031-9422(00)90266-8.
505 Chen, S., Fang, L., Xi, H., Guan, L., Fang, J., Liu, Y., et al. (2012). Simultaneous qualitative
506 assessment and quantitative analysis of flavonoids in various tissues of lotus (Nelumbo nucifera)
507 using high performance liquid chromatography coupled with triple quad mass spectrometry.
508 Anal Chim Acta. 724, 127-135. doi: 10.1016/j.aca.2012.02.051.
509 Chen, S., Xiang, Y., Deng, J., Liu, Y., and Li, S. (2013). Simultaneous analysis of anthocyanin
510 and non-anthocyanin flavonoid in various tissues of different lotus (Nelumbo) cultivars by
511 HPLC-DAD-ESI-MS(n). PLoS One. 8(4), e62291. doi: 10.1371/journal.pone.0062291.
512 Deng, J., Chen, S., Yin, X., Wang, K., Liu, Y., Li, S., et al. (2013). Systematic qualitative and
513 quantitative assessment of anthocyanins, flavones and flavonols in the petals of 108 lotus
514 (Nelumbo nucifera) cultivars. Food Chem. 139(1-4), 307-312. doi:
515 10.1016/j.foodchem.2013.02.010.
516 Deng, J., Fu, Z., Chen, S., Damaris, R.N., Wang, K., Li, T., et al. (2015). Proteomic and
517 epigenetic analyses of lotus (Nelumbo nucifera) petals between red and white cultivars. Plant
518 Cell Physiol. 56(8), 1546-1555. doi: 10.1093/pcp/pcv077.
519 Deng, S., Deng, Z., Fan, Y., Li, J., Liu, R., and Xiong, D. (2009). Application of high-speed
520 counter-current chromatography coupled with high performance liquid chromatography for the
521 separation and purification of Quercetin-3-O-sambubioside from the leaves of Nelumbo nucifera.
522 Front. Chem. Eng. China. 3(4), 375. doi: 10.1007/s11705-009-0247-9.
523 Gonnet, J.-F. (1998). Colour effects of co-pigmentation of anthocyanins revisited—1. A
524 colorimetric definition using the CIELAB scale. Food Chem. 63(3), 409-415. doi:
525 10.1016/S0308-8146(98)00053-3.

526 Gonnet, J.-F. (1999). Colour effects of co-pigmentation of anthocyanins revisited—2.A

527 colorimetric look at the solutions of cyanin co-pigmented byrutin using the CIELAB scale. Food

528 Chem. 66(3), 387-394. doi: 10.1016/S0308-8146(99)00088-6.

529 Goo, H.R., Choi, J.S., Na, D.H. (2009). Simultaneous determination of quercetin and its

530 glycosides from the leaves of Nelumbo nucifera by reversed-phase high-performance liquid

531 chromatography. Arch Pharm Res. 32, 201-206. doi: 10.1007/s12272-009-1136-y.

532 Guo, H. (2009). Cultivation of lotus (Nelumbo nucifera Gaertn. ssp. nucifera) and its utilization

533 in China. Genet Resour Crop Evol. 56(3), 323-330. doi: 10.1007/s10722-008-9366-2.

534 Han, Y., Wang, X., Chen, W., Dong, M., Yuan, W., Liu, X., et al. (2013). Differential expression

535 of carotenoid-related genes determines diversified carotenoid coloration in flower petal of

536 Osmanthus fragrans. Tree Genetics & Genomes. 10(2), 329-338. doi: 10.1007/s11295-013-0687-

537 8.

538 He, Q., Shen, Y., Wang, M., Huang, M., Yang, R., Zhu, S., et al. (2011). Natural variation in

539 petal color in Lycoris longituba revealed by anthocyanin components. PLoS One. 6(8), e22098.

540 doi: 10.1371/journal.pone.0022098.

541 Hyun, S.K., Yu, J.J., Chung, H.Y., Jung, H.A., and Choi, J.S. (2006). Isorhamnetin glycosides

542 with free radical and ONOO-scavenging activities from the stamens of Nelumbo nucifera. Arch

543 Pharm Res. 29(4), 287-292. doi: 10.1007/bf02968572.

544 Jeong, S.T., Goto-Yamamoto, N., Hashizume, K., and Esaka, M. (2006). Expression of the

545 flavonoid 3' -hydroxylase and flavonoid 3' ,5' -hydroxylase genes and flavonoid composition in

546 grape (Vitis vinifera). Plant Sci. 170(1), 61-69.

547 Jin, Z.M., He, J.J., Bi, H.Q., Cui, X.Y., and Duan, C.Q. (2009). Phenolic compound profiles in

548 berry skins from nine red wine grape cultivars in northwest China. Molecules. 14(12), 4922-

549 4935. doi: 10.3390/molecules14124922.

550 Jung, H.A., Jung, Y.J., Yoon, N.Y., Jeong, D.M., Bae, H.J., Kim, D.W., et al. (2008). Inhibitory

551 effects of Nelumbo nucifera leaves on rat lens aldose reductase, advanced glycation endproducts

552 formation, and oxidative stress. Food Chem Toxicol. 46(12), 3818-3826. doi:

553 10.1016/j.fct.2008.10.004.

554 Jung, H.A., Kim, J.E., Chung, H.Y., and Choi, J.S. (2003). Antioxidant principles of Nelumbo

555 nucifera stamens. Arch Pharm Res. 26(4), 279-285. doi: 10.1007/BF02976956.

556 Juranić, Z., and Žižak, Ž. (2005). Biological activities of berries: from antioxidant capacity to

557 anti-cancer effects. BioFactors. 23(4), 207-211. doi: 10.1002/biof.5520230405.

558 Li, C., Wang, L., Shu, Q., Xu, Y., and Zhang, J. (2008). Pigments composition of petals and

559 floral color change during the blooming period in Rhododendron mucronulatum. Acta

560 Horticulture Sinica. 35, 1023-1030. doi: 10.3724/SP.J.1005.2008.01083.

561   Li, S., Wu, Q., Yuan, R., Shao, S., Zhang, H., and Wang, L. (2014a). Recent advances in

562   metabolic products of flavonoids in Nelumbo. Chin. Bull. Bot. 49(6), 738. doi:

563   10.3724/SP.J.1259.2014.00738.

564   Li, S.S., Wu, J., Chen, L.G., Du, H., Xu, Y.J., Wang, L.J., et al. (2014b). Biogenesis of C-

565   glycosyl flavones and profiling of flavonoid glycosides in lotus (Nelumbo nucifera). PLoS One.

566   9(10), e108860. doi: 10.1371/journal.pone.0108860.

567   Li, Y., Yang, S., Gao, B., and Fu, X. (2011). Co-pigmentation effect and color stability of

568   flavonoids on red dayberry (Myrica rubra Sieb. et Zucc) Anthocyanins. Food Science. 32(13),

569   37-39. doi: 10.1631/jzus.B1000185.

570   Lim, S.S., Jung, Y.J., Hyun, S.K., Lee, Y.S., and Choi, J.S. (2006). Rat lens aldose reductase

571   inhibitory constituents of Nelumbo nucifera stamens. Phytother Res. 20(10), 825-830. doi:

572   10.1002/ptr.1847.

573   Lin, L.-Z., and Harnly, J.M. (2007). A screening method for the identification of glycosylated

574   flavonoids and other phenolic compounds using a standard analytical approach for all plant

575   materials. J Agric Food Chem. 55(4), 1084-1096. doi: 10.1021/jf062431s.

576   Mukherjee, P.K., Mukherjee, D., Maji, A.K., Rai, S., and Heinrich, M. (2009). The sacred lotus

577   (Nelumbo nucifera)–phytochemical and therapeutic profile. J Pharm Pharmacol. 61(4), 407-422.

578   doi: 10.1211/jpp.61.04.0001.

579   Noriko, N., Masako, F.M., Yuko, F., Kanako, I., Kenichi, S., Hideyuki, S., et al. (2010).

580   Generation of pink flower varieties from blue Torenia hybrida by redirecting the flavonoid

581   biosynthetic pathway from delphinidin to pelargonidin. Plant Biotechnology. 27, 375-383.

582   Nishihara, M., Nakatsuka, T. (2011). Genetic engineering of flavonoid pigments to modify

583   flower

584   color in floricultural plants. Biotechnol Lett. 33, 433-441. doi: 10.1007/s10529-010-0461-z.

585   Nováková, L., Matysová, L., and Solich, P., (2006). Advantages of application of UPLC in

586   pharmaceutical analysis. Talanta. 68(3), 908-918. doi: 10.1016/j.talanta.2005.06.035.

587   Pfeiffer, P., Hegedűs, A. (2011). Review of the molecular genetics of flavonoid biosynthesis in

588   fruits. Acta Aliment. 40, 150-163. doi: 10.1556/AAlim.40.2011.Suppl.15. doi:

589   10.1556/aalim.40.2011.suppl.15.

590   Schwinn, K., Venail, J., Shang, Y., Mackay, S., Alm, V., Butelli, E., et al. (2006). A small family

591   of MYB-regulatory genes controls floral pigmentation intensity and patterning in the genus

592   Antirrhinum. Plant Cell. 18(4), 831-851. doi: 10.2307/20076645.

593   Sharma, B.R., Gautam, L.N., Adhikari, D., and Karki, R. (2017). A comprehensive review on

594   chemical profiling of Nelumbo Nucifera: potential for drug development. Phytother Res. 31(1),

595   3-26. doi: 10.1002/ptr.5732.

596 Stafford, H.A. (1998). Teosinte to maize - Some aspects of missing biochemical and
597 physiological data concerning regulation of flavonoid pathways. Phytochemistry. 49(2), 285-
598 293. doi: 10.1016/S0031-9422(98)00175-7.

599 Sun, S.S., Gugger, P.F., Wang, Q.F., and Chen, J.M. (2016). Identification of a R2R3-MYB gene
600 regulating anthocyanin biosynthesis and relationships between its variation and flower color
601 difference in lotus (Nelumbo Adans.). PeerJ. 4, e2369. doi: 10.3724/sp.J.1259.2014.00738.

602 Sun, W., Li, C.H., Wang, L.S., Dai, S.L., and Xu, Y.J. (2009). Anthocyanins present in flowers
603 of senecio cruentus with different colors. Acta Horticulture Sinica. 36(12), 1775-1782.

604 Suzuki, H., Sasaki, R., Ogata, Y., Nakamura, Y., Sakurai, N., Kitajima, M., et al. (2008).
605 Metabolic profiling of flavonoids in Lotus japonicus using liquid chromatography Fourier
606 transform ion cyclotron resonance mass spectrometry. Phytochemistry. 69(1), 99-111. doi:
607 10.1016/j.phytochem.2007.06.017.

608 Wang, L.S., Shiraishi, A., Hashimoto F., Aoki, N., Shimizu, K., and Sakata Y., (2001). Analysis
609 of Petal Anthocyanins to Investigate Flower Coloration of Zhongyuan (Chinese) and Daikon
610 Island (Japanese) Tree Peony Cultivars. J. Plant Res. 114, 33-43.

611 Yamagishi, M., Shimoyamada, Y., Nakatsuka, T., and Masuda, K. (2010). Two R2R3-MYB
612 genes, homologs of Petunia AN2, regulate anthocyanin biosyntheses in flower Tepals, tepal
613 spots and leaves of asiatic hybrid lily. Plant Cell Physiol. 51(3), 463-474. doi:
614 10.1093/pcp/pcq011.

615 Yang, R.Z., Wei, X.L., Gao, F.F., Wang, L.S., Zhang, H.J., Xu, Y.J., et al. (2009). Simultaneous
616 analysis of anthocyanins and flavonols in petals of lotus (Nelumbo) cultivars by high-
617 performance liquid chromatography-photodiode array detection/electrospray ionization mass
618 spectrometry. J Chromatogr A. 1216(1), 106-112. doi: 10.1016/j.chroma.2008.11.046.

619 Zhang, J., Wang, L.S., Gao, J.M., Li, S.B.,Xu, Y.J., Li, C.H., et al. (2011a). Identification of
620 anthocyanins involving in petal coloration in Chaenomeles speciosa cultivars. Acta Horticulture
621 Sinica. 38(3), 527-534.

622 Zhang, Z., Song, J., Wang, Z.Y., Zhao, X., and Wang, Y.J. (2011b). Effect of co-pigments on
623 enhancing stability of anthocyanins from Lonicera edulis Turcz. Sci Tech Food Ind. 4, 092. doi:
624 10.1097/RLU.0b013e3181f49ac7.

625 Zhao, D., and Tao, J. (2015). Recent advances on the development and regulation of flower color
626 in ornamental plants. Front Plant Sci. 6, 261. doi: 10.3389/fpls.2015.00261.

627 Zhao, D., Tao, J., Han, C., and Ge, J. (2012). Flower color diversity revealed by differential
628 expression of flavonoid biosynthetic genes and flavonoid accumulation in herbaceous peony
629 (Paeonia lactifloraPall.). Mol Biol Rep. 39(12), 11263-11275. doi: 10.1007/s11033-012-2036-7.

630 Zhu, C., Bai, C., Sanahuja, G., Yuan, D., Farre, G., Naqvi, S., et al. (2010). The regulation of

631 carotenoid pigmentation in flowers. Arch Biochem Biophys. 504(1), 132-141. doi:

632 10.1016/j.abb.2010.07.028.

633 Zhu, M., Zheng, X., Shu, Q., Li, H., Zhong, P., Zhang, H., et al. (2012). Relationship between

634 the composition of flavonoids and flower colors variation in tropical water lily (Nymphaea)

635 cultivars. PLoS One. 7(4), e34335. doi: 10.1371/journal.pone.0034335.

636 Zhu, Y., Ling, W., Guo, H., Song, F., Ye, Q., Zou, T., et al. (2013). Anti-inflammatory effect of

637 purified dietary anthocyanin in adults with hypercholesterolemia: a randomized controlled trial.

638 Nutr Metab Cardiovasc Dis. 23(9), 843-849. doi: 10.1016/j.numecd.2012.06.005.

Supplementary material

640 **Supplementary Table S1.** Sacred lotus cultivars used in this study.

641 **Supplementary Figure S1.** Relative content (%) of different anthocyanins contributing to the

642 total anthocyanins (A) and relative content (%) of different non-anthocyanin flavonoids

643 contributing to the total non-anthocyanin flavonoids (B) in 207 lotus cultivars. The numbers (x-

644 axis) in the figure represent sample numbers, which correspond to cultivars in Supplementary

645 Table S1.

646 **Supplementary Table S2.** The primer information of the three structural genes.

647

Identification of flavonoids in petals of lotus.

[a] Rt: retention time on C_{18} column. [b] Compounds identified by standards. [c] Compounds identified for the first in sacred lotus.

Table 1. Identification of flavonoids in petals of lotus.

Peak No.	Rt(min)[a]	λmax (nm)	Parent ion(m/z)(measured value)	Molecular fomular	Parent ion(m/z) (calculated value)	Error (ppm)	Fragmentation profile(m/z) (Relative abundance %)	Identification	References
1	4.765	523.9, 272.2	463.0904[M-2H]$^-$	$C_{21}H_{21}O_{12}^+$	463.0882	-4.75	301.0376(100),300.0358(95.28)	delphinidin 3-O-glucoside(Dp-3-Glu)	(Yang et al., 2009)
2	5.959	519.0, 279.3	447.0951[M-2H]$^-$	$C_{21}H_{21}O_{11}^+$	447.0933	-4.03	285.0448(100),284.0372(57.11)	cyanidin 3-O-glucoside(Cy-3-Glu)	(Yang et al., 2009)
3	6.770	523.9, 279.3	477.1046[M-2H]$^-$	$C_{22}H_{23}O_{12}^+$	477.1038	-1.68	315.0547(100),314.0485(87.66)	petunidin 3-O-glucoside(Pt-3-Glu)[b]	(Yang et al., 2009)
4	8.418	517.8, 279.3	461.1099[M-2H]$^-$	$C_{22}H_{23}O_{11}^+$	461.1089	-2.17	299.0597(100),298.0519(55.27)	peonidin 3-O-glucoside(Pn-3-Glu)	(Yang et al., 2009)
5	9.271	527.6, 277.0	491.1208[M-2H]$^-$	$C_{23}H_{25}O_{12}^+$	491.1195	-2.65	329.0711(100),328.0644(69.32)	malvidin 3-O-glucoside(Mv-3-Glu)	(Yang et al., 2009)
6	11.591	355.4, 264.7	493.0640[M-H]$^-$	$C_{21}H_{18}O_{14}$	493.0624	-3.25	317.0418(100),318.0451(24.47)	myricetin 3-O-glucuronide(Myr-3-Gln)	(Deng et al., 2013)
7	12.268	356.6, 252.0	595.1309[M-H]$^-$	$C_{26}H_{28}O_{16}$	595.1305	-0.67	300.0380(100),301.0433(21.23)	quercetin 3-O-sambubioside(Qc-3-Sam/Qc-3-Xyl-Glu)	(Deng et al., 2009)
8	12.606	356.6, 253.2	623.1475[M-H]$^-$	$C_{27}H_{27}O_{17}$	623.1254	-11.72	301.0467(100),302.0502(13.95),446.7323(2.46)	quercetin 3-O-pentose-glucuronide(Qc-3-Pen-Gln)[c]	(Ablajan et al., 2006)

9	14.349	319.9, 252.0	463.0910[M-H]-	$C_{21}H_{20}O_{12}$	463.0882	-6.05	301.0362(100),300.0251(20.05)	quercetin 7-O-glucoside(Qc-7-Glu)[c]	(Ablajan et al., 2006)
10	14.687	352.9, 268.6	609.1463[M-H]-	$C_{27}H_{30}O_{16}$	609.1461	-0.33	609.1461(100),300.0276(50.58),301.0325(36.65)	quercetin 3-O-neohesperidoside(Qc-3-Neo)	(Li et al., 2014b)
11	15.399	354.1, 254.4	463.0900[M-H]-	$C_{21}H_{20}O_{12}$	463.0882	-3.89	300.0274(100),301.0343(64.38)	quercetin 3-O-galactoside(Qc-3-Gal/hyperoside)[b]	(Suzuki et al., 2008)
12	15.913	352.9, 255.5	477.0690[M-H]-	$C_{21}H_{18}O_{13}$	477.0675	-3.14	301.0369(100),302.0394(23.85)	quercetin 3-O-glucuronide (Qc-3-Gln)	(Yang et al., 2009)
13	16.377	356.5, 252.0	493.0995[M-H]-	$C_{22}H_{22}O_{13}$	493.0988	-1.42	330.0482(100),331.0518(56.74),315.0228(19.51)	laricitrin 3-O-hexose(Lar-3-Hex)[c]	(Jin et al., 2009)
14	16.663	359.0, 252.0	507.0788[M-H]-	$C_{22}H_{20}O_{14}$	507.078	-1.58	331.0581(100),332.0569(22.80),316.0341(8.97)	laricitrin 3-O-glucuronide(Lar-3-Gln)[c]	(Jin et al., 2009)
15	17.263	343.5, 252.0	593.1516[M-H]-	$C_{27}H_{30}O_{15}$	593.1512	-0.67	593.1740(100),284.0420(76.83),285.0471(42.92)	Kaempferol 3-O-neohesperidoside(Kae-3-Neo/Kae-3-Rha-Glu)	(Lim et al., 2006; Sharma et al., 2017)
16	18.374	343.5, 265.1	447.0952[M-H]-	$C_{21}H_{20}O_{11}$	447.0933	-4.25	284.0428(100),284.0492(45.53)	kaempferol 3-O-galactoside(Kae-3-Gal)	(Jung et al., 2003)
17	18.870	343.5, 253.2	593.1516[M-H]-	$C_{27}H_{30}O_{15}$	593.1512	-0.67	285.0500(100),284.042(52.21)	kaempferol 3-O-rutinoside(Kae-3-Rut)	(Hyun et al., 2017; Sharma et al., 2017)
18	19.259	352.9,	623.1612[M-H]-	$C_{28}H_{32}O_{16}$	623.1618	0.96	623.1839(100),315.0625(52.24),314.0563(28.1	isorhamnetin 3-O-rutinoside (Iso-3-Rut)	(Yang et al., 2009)

		253.2					2)		
19	19.770	347.0, 265.1	447.0951[M-H]$^-$	$C_{21}H_{20}O_{11}$	447.0933	-4.03	284.0324(100),285.0499(60.54)	kaempferol 3-O-glucoside(Kae-3-Glu/astragalin)^b	(Chen et al., 2012; Yang et al., 2009)
20	20.536	356.6, 253.2	507.1157[M-H]$^-$	$C_{23}H_{24}O_{13}$	507.1144	-2.56	344.0694(100),345.0747(39.53)	syringetin 3-O-hexose(Syr-3-Hex)	(Guo, 2009)
21	20.821	356.6, 253.2	477.1051[M-H]$^-$	$C_{22}H_{22}O_{12}$	477.1038	-2.72	314.0554(100),315.0595(27.71)	isorhamnetin 3-O-glucoside(Iso-3-Glu)^b	(Sharma et al., 2017)
22	21.377	351.7, 253.2	491.0845[M-H]$^-$	$C_{22}H_{20}O_{13}$	491.0831	-2.85	315.0522(100),316.0567(28.44)	isorhamnetin 3-O-glucuronide (Iso-3-Gln)	(Chen et al., 2012)
23	21.617	357.8, 252.0	521.0960[M-H]$^-$	$C_{23}H_{22}O_{14}$	521.0937	-4.41	345.0607(100),346.0639(29.29)	syringetin 3-O-glucuronide(Syr-3-Gln)	(Li et al., 2014b)

2 ^{a} Rt: retention time on C_{18} column.

3 ^{b} Compounds identified by standards.

4 ^{c} Compounds identified for the first in sacred lotus.

Average content (ug g^{-1} fresh weight) of different pigment types in different colors of lotus.

[*] TA=the total content of the five anthocyanins; TF=the total content of the six non-anthocyanin flavonoid derivatives; [#] Each value presents the mean ± standard deviation (SD) of three independent replicates. Different letters represent significant (P < 0.05) differences between means according to analysis of variance (ANOVA) combined with Duncan's multiple range test. And the differences are within the row.

1 **Table 2.** Average content (ug g^{-1} fresh weight) of different pigment types in different colors of lotus.

Type	Compound	Purple-red	Red	Yellow	White
Anthocyanins	Dp-3-Glu	88.93±6.37a[#]	28.86±4.54b	0.31±0.31c	1.74±0.49c
	Cy-3-Glu	38.73±2.19a	22.00±3.29b	0.62±0.43c	1.14±0.40c
	Pt-3-Glu	61.13±2.90a	19.66±1.85b	0.58±0.40c	1.84±0.48c
	Pn-3-Glu	44.05±1.88a	22.16±1.94b	0.71±0.50c	1.28±0.46c
	Mv-3-Glu	231.64±10.27a	79.06±10.27b	1.46±0.68c	4.36±0.92c
	TA[*]	464.47±19.29a	171.74±19.41b	3.67±2.10c	10.36±2.44c
Non-anthocyanin flavonoids	Quercetin derivatives	762.17±33.76c	1283.71±205.09b	2254.58±229.40a	950.51±104.46c
	Kaempferol derivatives	732.82±42.43a	749.44±80.60a	566.21±69.88a	731.88±55.60a
	Isorhamnetin derivatives	129.55±5.89b	173.74±22.86b	319.84±43.77a	194.34±14.45ab
	Syringetin derivatives	18.72±0.76b	21.98±2.68b	82.99±10.97a	49.18±5.52a
	Myricetin derivatives	79.62±3.70b	92.44±11.79b	217.35±37.52a	80.96±9.47b
	Laricitrin derivatives	36.29±2.29b	39.72±4.48b	76.95±9.29a	39.30±2.66b
	TF[*]	1759.17±68.07c	2361.02±269.12b	3517.93±289.08a	2046.18±133.87bc

2 [*] TA=the total content of the five anthocyanins; TF=the total content of the six non-anthocyanin flavonoid derivatives;

3   # Each value presents the mean ± standard deviation (SD) of three independent replicates. Different letters represent significant (P <

4   0.05) differences between means according to analysis of variance (ANOVA) combined with Duncan's multiple range test. And the

5   differences are within the row.

Average content (ug g^{-1} fresh weight) of different pigment types in different colors of lotus.

[*] TA=the total content of the five anthocyanins; TF=the total content of the six non-anthocyanin flavonoid derivatives; [#] Each value presents the mean ± standard deviation (SD) of three independent replicates. Different letters represent significant (P < 0.05) differences between means according to analysis of variance (ANOVA) combined with Duncan's multiple range test. And the differences are within the row.

Table 2. Average content (ug g^{-1} fresh weight) of different pigment types in different colors of lotus ~~(each value is the mean ± standard deviation~~mean ± SD).

Type	Compound	Purple-red	Red	Yellow	White
Anthocyanins	Dp-3-Glu	88.93±6.37a[#]	28.86±4.54b	0.31±0.31c	1.74±0.49c
	Cy-3-Glu	38.73±2.19a	22.00±3.29b	0.62±0.43c	1.14±0.40c
	Pt-3-Glu	61.13±2.90a	19.66±1.85b	0.58±0.40c	1.84±0.48c
	Pn-3-Glu	44.05±1.88a	22.16±1.94b	0.71±0.50c	1.28±0.46c
	Mv-3-Glu	231.64±10.27a	79.06±10.27b	1.46±0.68c	4.36±0.92c
	TA[*]	464.47±19.29a	171.74±19.41b	3.67±2.10c	10.36±2.44c
Non-anthocyanin flavonoids	Quercetin derivatives	762.17±33.76c	1283.71±205.09b	2254.58±229.40a	950.51±104.46c
	Kaempferol derivatives	732.82±42.43a	749.44±80.60a	566.21±69.88a	731.88±55.60a
	Isorhamnetin derivatives	129.55±5.89b	173.74±22.86b	319.84±43.77a	194.34±14.45ab
	Syringetin derivatives	18.72±0.76b	21.98±2.68b	82.99±10.97a	49.18±5.52a
	Myricetin derivatives	79.62±3.70b	92.44±11.79b	217.35±37.52a	80.96±9.47b
	Laricitrin derivatives	36.29±2.29b	39.72±4.48b	76.95±9.29a	39.30±2.66b
	TF[*]	1759.17±68.07c	2361.02±269.12b	3517.93±289.08a	2046.18±133.87bc

[*] TA=the total content of the five anthocyanins; TF=the total content of the six non-anthocyanin flavonoid derivatives;

4 [#] Each value presents the mean ± standard deviation (SD) of three independent replicates. Different letters represent significant ($P <$

5 0.05) differences between means according to analysis of variance (ANOVA) combined with Duncan's multiple range test. And the

6 differences are within the row.

Figure 1

Chromatograms and MS spectrum of flavonoids detected in lotus petals.

(A) HPLC chromatograms of anthocyanins at 520 nm (peaks 1-5) and of non-anthocyanin flavonoids at 350 nm (peaks 6-23). Peak numbers in this figure correspond to compound numbers in Table 1. And these data were obtained from the mixture of three cultivars: "Qiaoshou-I" (71), "Jinlingningcui" (151), and "Silian13-I" (178). (B-D) Structures of four flavonoids found in lotus petals. MS/MS spectra (in NI mode) of quercetin 3-*O*-pentose-glucuronide (B, **8**), quercetin 7-*O*-glucoside (C, **9**), laricitrin 3-*O*-hexose (D, **13**), and laricitrin 3-*O*-glucuronide (E, **14**), and produced by each precursor.
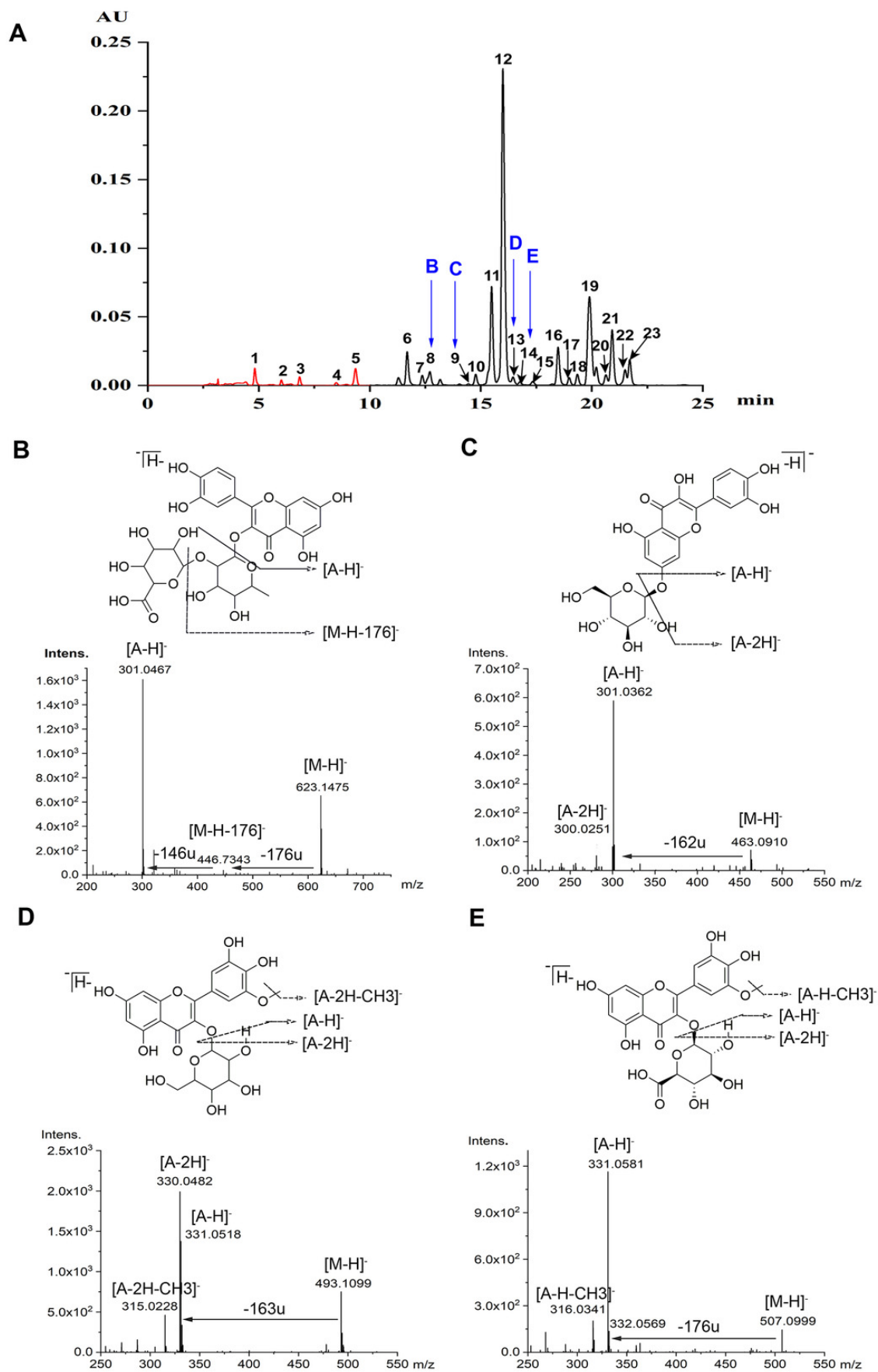
Figure 2

The average content (ug g^{-1} fresh weight) of each anthocyanin compound

(A) and each non-anthocyanin flavonoid compound (B) in 207 lotus cultivars. The numbers (x-axis) in the figure represent sample numbers, which correspond to the cultivars in Supplementary Table S1.
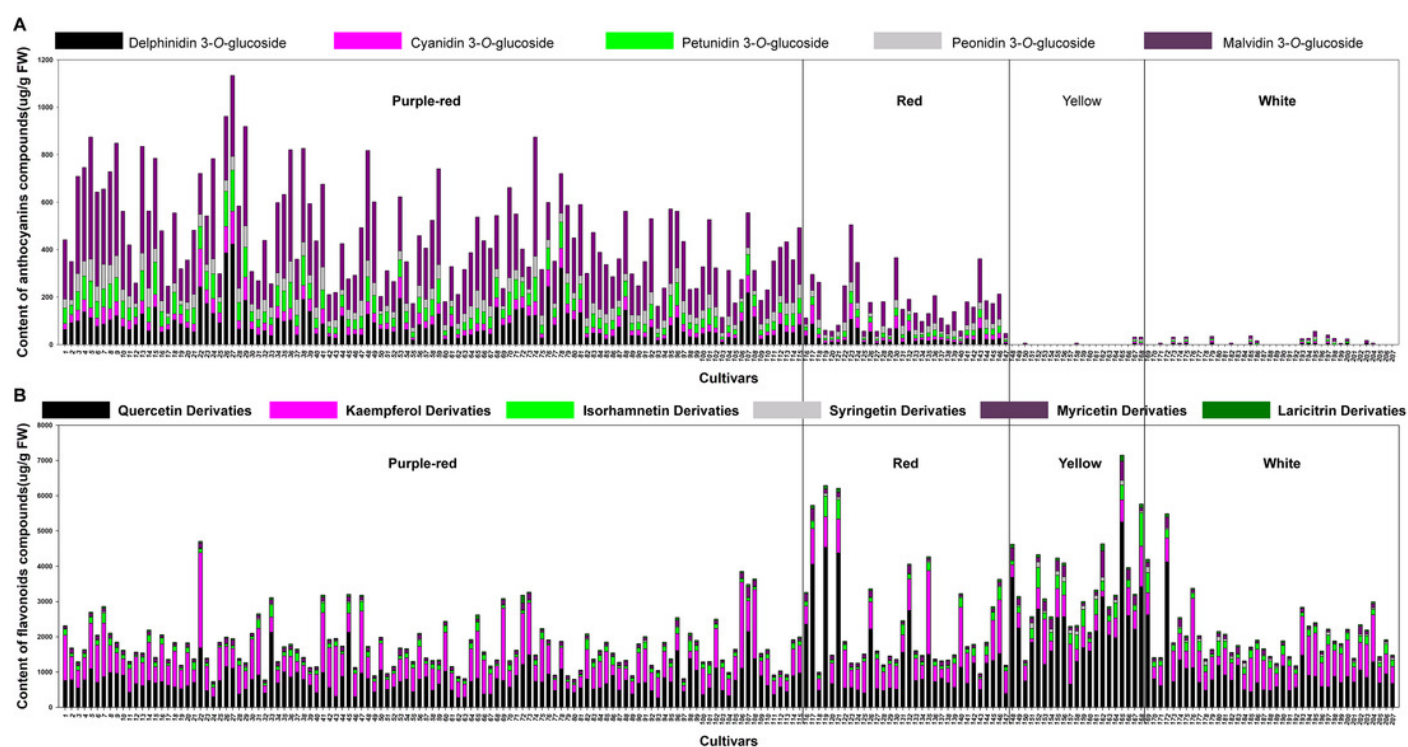
Figure 3

A heat map of the individual anthocyanin and non-anthocyanin flavonoid contents.

The row values represent the Z-score normalization of the concentration of identified flavonoids and the column represents the tested samples. The numbers on the top line correspond to cultivar numbers in Supplementary Table S1. Red represents relatively high concentration and blue represents relatively low concentration of the identified flavonoids in petals of each lotus cultivar.

Chemistry Journals
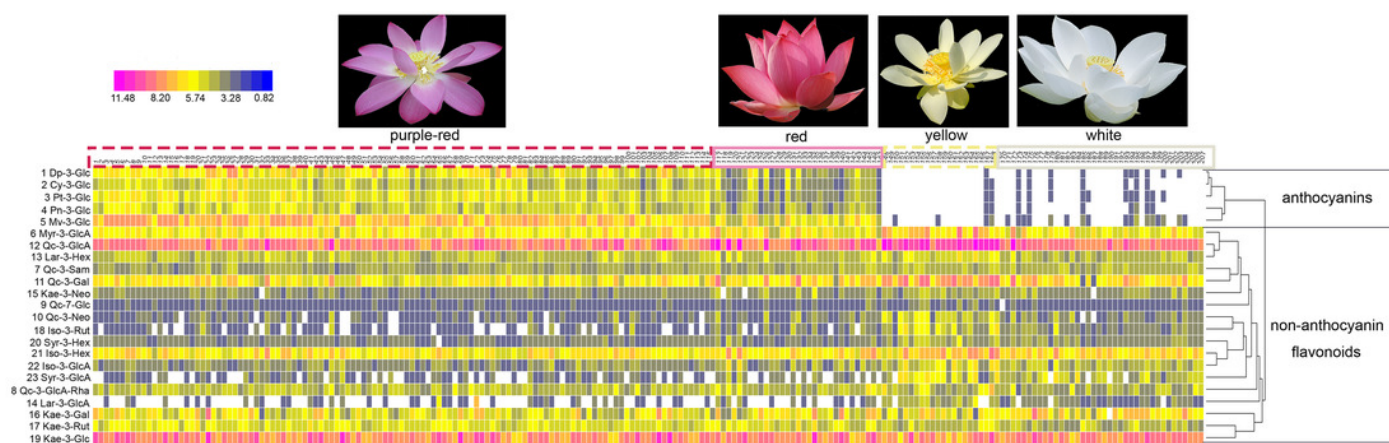
Figure 4

A heat map of correlation matrix of color parameters and 23 compounds from petals of 207 lotus cultivars.

Each square indicates Pearson's correlation coefficient for a pair of data, and the intensity of red and green colors in the heat map indicates the level of positive and negative correlation, respectively.

![PeerJ] **Chemistry Journals**
Analytical, Inorganic, Organic, Physical, Materials Science
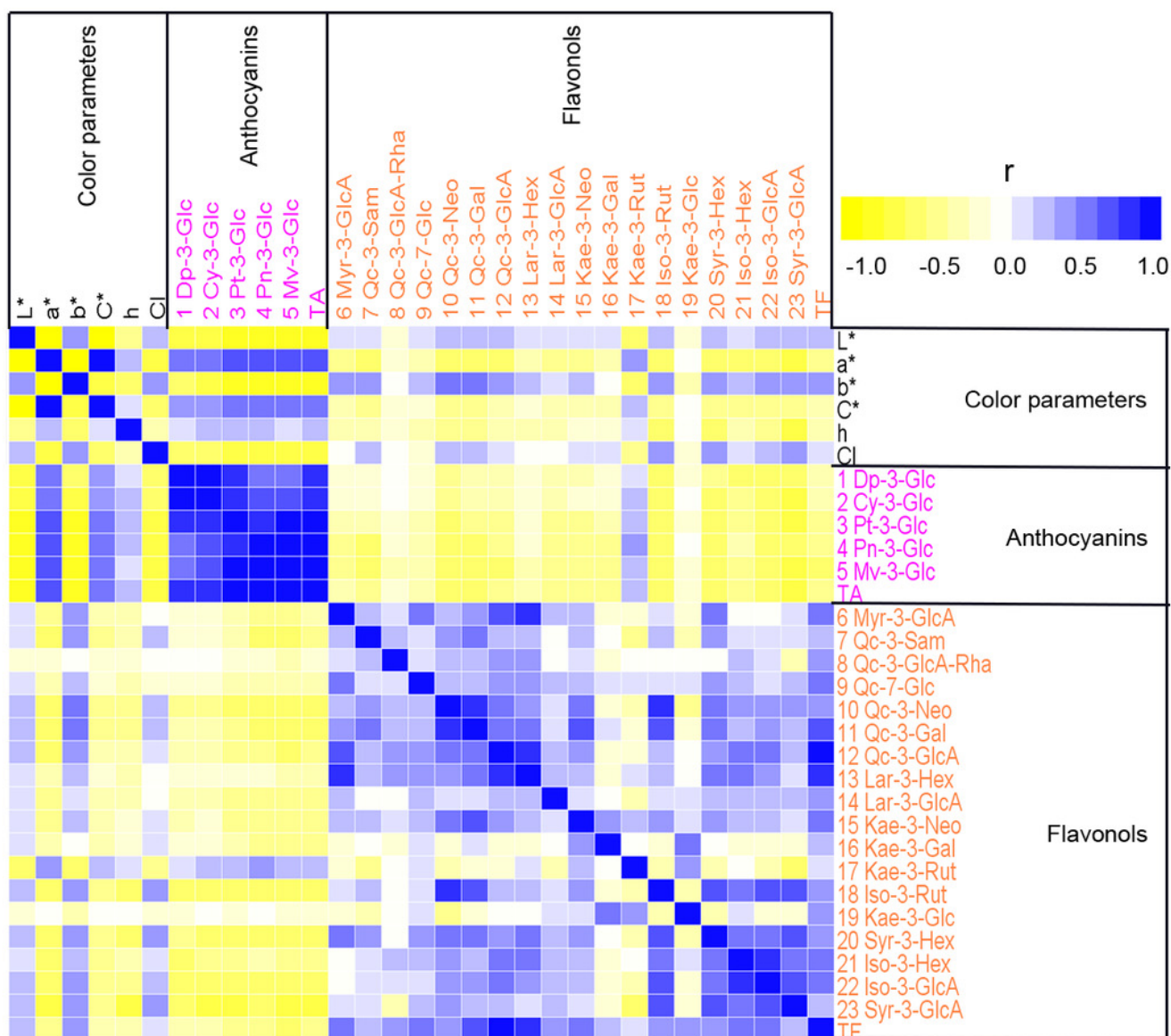
Figure 5

The deduced biosynthesis pathway of flavonoids in lotus petals.

CoA: acethl coenzyme A; CHS: chalcone synthase; CHI: chalcone isomerase; F3H: flavonoid 3-hydroxylase; F3'H: flavonoid 3'-hydroxylase; F3'5'H: flavonoid 3'5'-hydroxylase; DFR: dihydroflavonol reductase; ANS: anthocyanidin synthase; FLS: flavonol synthase; UFGT: UDP flavonoid glycosyltransferase; OMT: O-methyltransferase.
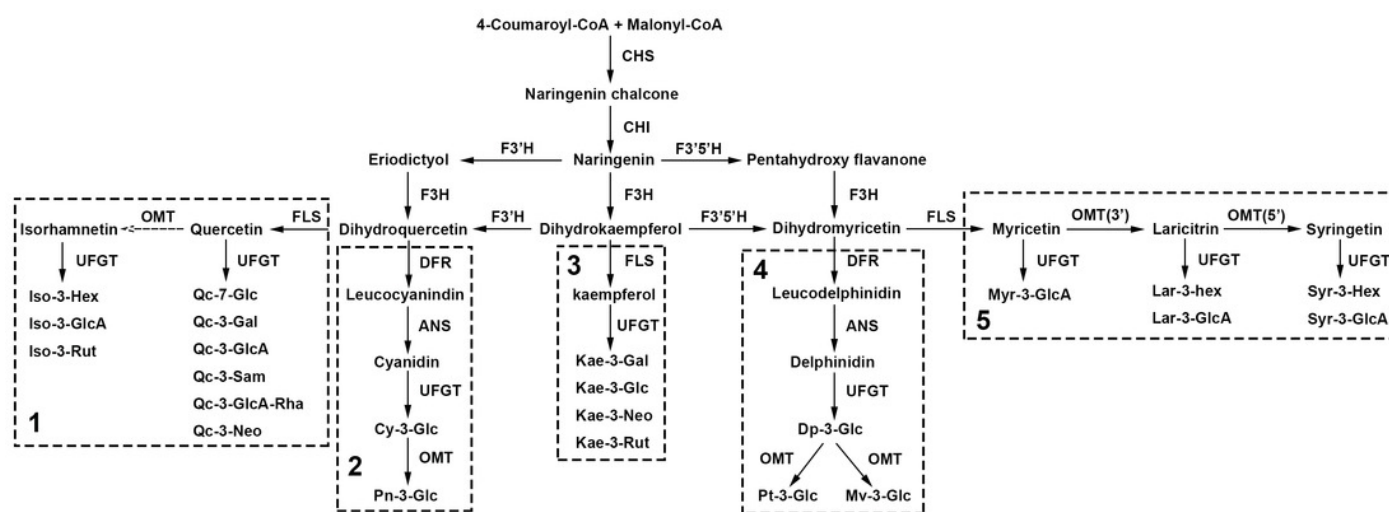
Figure 6

The expression profile of three structural genes (DFR, UFGT and OMT) in three *Nelumbo* cultivars (B88, A89, B121) was determined by qRT-PCR.